Optimal quantised bits for estimation over a capacity and power limited, lossy channel

Venkatareddy Akumalla ✉
and Mohammed Zafar Ali Khan
Department of Electrical Engineering, Indian Institute of Technology Hyderabad, Sangareddy, Hyderabad, India
✉ Email: ee13p0010@iith.ac.in

This letter considers the problem of estimating the state of a scalar dynamical system over a wireless channel that is lossy, capacity, and power limited. The limited power assumption, which is valid for most real problems, links the number of quantisation bits and packet error rate. As the number of quantisation bits increases, the quantisation noise decreases but the packet loss rate increases. It is shown that the estimation error variance (EEV) is minimised for a range of quantisation bits. Further, it is shown that operating beyond the optimal range sharply increases the EEV. Simulation results corroborating the analytical results are also presented.

Introduction: Control and estimation of cyber physical systems (CPS) involve wireless communication as it is flexible, cheap, and easy to use. Wireless systems are capacity and power limited and hence lossy. Data transmitted through a wireless system may suffer from quantisation noise and packet loss. So, many researchers have tried to solve problems associated with CPS. These include optimal linear quadratic Gaussian (LQG) control subject to quantisation noise and packet loss [1], LQG control subject to the packet delay [2], Kalman filtering (KF) in wireless sensor networks [3], and KF with quantised measurements (quantised KF) [4, 5]. The remote KF with 1-bit quantisation has been introduced in [6] and then extended to remote Kalman filtering for multi-bits in [7]. For remote linear estimation, the optimal linear encoder for uniform quantiser was devised in [8], and simultaneous design of the encoder and the quantiser was presented in [9]. KF with transmit power constraint have been addressed in [10–15]. However, these works consider the quantisation noise and packet loss rate as independent.

In this letter, we propose remote estimation of a linear scalar CPS; in a capacity and power-limited, lossy channel. In this model, the encoded data are quantised (b bits/sample), encoded using a modulation and coding scheme (MCS), and transferred from the transmitter to the receiver over a lossy wireless channel. This transfer is typically modelled by an independent Bernoulli packet loss process when the channel is capacity limited [16, 17]. This modelling decouples the quantisation noise and packet error rate and is justified because any degradation in packet loss rate due to increased data rate can be compensated by an increase in power. A capacity-limited and power-limited channel does not offer this luxury, and an increase in data rate due to more quantisation bits increases the packet loss rate (PLR). We show that in such a channel, there is a range of quantised bits in which the EEV is minimised. We characterise this optimal number of quantised bits and study them in various simulation environments. It is observed that the EEV sharply increases when operating outside the optimal range.

System model: We consider a scalar discrete-time linear state dynamical system, given by

$$x_{k+1} = a\,x_k + w_k\,, \tag{1}$$

where x_k is the system state and w_k is the system state noise at time instant k. The measurement of the system at time k, is given by

$$y_k = c\,x_k + v_k\,, \tag{2}$$

where y_k and v_k are the system observation and the measurement noise at time instant k. Variables a and c are the scalar system and the scalar measurement coefficients, respectively. For a stable system $|a| < 1$ and we assume that the measurement is scaled so that $c = 1$.

An encoder $f(\cdot)$ encodes the data to u_k which is quantised to $q(u_k)$. This quantised signal $q(u_k)$ is transmitted using a modulation and coding scheme (MCS) that encodes the data at a rate R, provides a coding gain

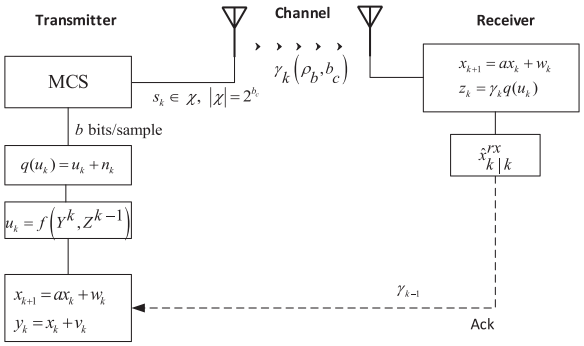

Fig. 1 *A schematic model of the remote estimation system*

C and transmits a signal, s_k from a constellation $\chi, |\chi| = 2^{b_c}$, where $b_c = b/R$. The received data suffers from packet loss at time instant k denoted as ($\gamma_k \in \{0, 1\}$), as shown in Figure 1. The extended system model together with the encoder and quantiser at the receiver side can be represented as

$$x_{k+1} = ax_k + w_k, u_k = f\left(y^k, z^{k-1}\right), z_k = \gamma_k q\left(u_k\right) = \gamma_k\left(u_k + n_k\right) \tag{3}$$

where the sequences $\mathcal{Y}^k = \{y_l\}_{l=0}^{l=k}$, $\mathcal{Z}^{k-1} = \{z_l\}_{l=0}^{l=k-1}$, and where $n_k \sim \mathcal{N}(0, \sigma_{n_k}^2)$ is the quantisation noise, which following [9, 10, 17] is assumed to be white Gaussian. The probability of packet loss γ_k depends on the MCS scheme chosen and in-particular depends on the signal to noise ratio per bit, ρ_b, and the number of coded bits per sample $b_c = b/R$ as shown in Figure 1. We assume that acknowledgement signals are exchanged, so that the packet loss sequence $\{\gamma_t\}_{t=0}^{t=k-1}$ is perfectly known at the transmitter and it can perfectly reconstruct $\mathcal{Z}^{k-1}$.

Also, the modelling is very general when $f(\cdot) = y$, then the system models quantisation of the observation vector. When $f(\cdot) = \hat{x}^{tx}_{k|k}$, the transmitted message is an estimate of the state at the transmitter and when $f(\cdot) = \hat{x}^{tx}_{k|k} - \hat{x}^{tx}_{k|k-1}$ where $\hat{x}^{rx}_{k|k-1} = \mathbb{E}\{x_k \mid \mathcal{Z}_{k-1}\}$ is the prediction at the receiver and $\mathbb{E}[\cdot]$ is the expectation operator. In what follows we assume the optimal encoding strategy of transmitting the innovation [7] for a uniform quantiser. The remote estimation is done for the extended system model to obtain $\hat{x}^{rx}_{k|k}$, and is given by

$$\hat{x}^{rx}_{k|k} = \mathbb{E}_\gamma\left[x_k \mid \mathcal{Z}^k\right]. \tag{4}$$

The remote estimate of the state is done to minimise the EEV at the receiver, defined as

$$p^{rx}_{k|k} = \mathbb{E}_\gamma\left[\left|x_k - \hat{x}^{rx}_{k|k}\right|^2\right]. \tag{5}$$

For the optimal coded system $u_k = \hat{x}^{tx}_{k|k} - \hat{x}^{rx}_{k|k-1}$, and the receiver error variance is given by [16]

$$p^{rx}_{t+1|t} = a^2 p^{rx}_{t|t-1} + \sigma_w^2 - (1-\epsilon)\frac{a^2\Lambda}{1+\Lambda}\left(p^{rx}_{t|t-1} - p^{tx}_{t|t}\right) \tag{6}$$

where $p^{tx}_{t|t}$ is the EEV at the transmitter, Λ denotes the signal to quantisation noise ratio (SQNR) and $\epsilon = \mathbb{P}(\gamma_k = 0)$ is the packet loss rate. Let $p^{tx}_{\infty} = \lim_{t\to\infty} p^{tx}_{t|t}$. Then the steady state EEV is given by [17]

$$p^{CF}(b_c) = \lim_{t\to\infty} p^{rx}_{t+1|t} = \frac{\sigma_w^2 + (1-\epsilon)\frac{a^2\Lambda}{\Lambda+1}p^{tx}_{\infty}}{1 - a^2\frac{1+\epsilon\Lambda}{1+\Lambda}}. \tag{7}$$

Problem formulation: In most analysis of Kalman filter in capacity-limited channels, the packet loss rate, $\epsilon = \mathbb{P}(\gamma_k = 0)$, is assumed to be independent of the number of quantisation bits, b. This is particularly true when there is no power constraint. Moreover, as the number of quantisation bits increase the power can be increased to get a desired ϵ. However, in practical systems, and in particular for power-limited systems, this is not possible. In such systems an increase in the number of quantisation bits results in a higher throughput and requires the use of a higher modulation scheme without a proportional increase in the SNR. This results in an increased bit error rate (BER) and hence an increased packet loss rate, ϵ. This suggests a trade-off that as the number of quantisation bits increase the quantisation noise decreases but results in an increased packet loss rate. In addition, even for capacity-limited

Table 1. Approximate bit error rates for coherent modulations

Modulation	$P_b(\rho_b)$
MPAM:	$P_b \approx \frac{2(M-1)}{M\log_2 M} Q\left(\sqrt{\frac{6\rho_b \log_2 M}{(M^2-1)}}\right)$
MPSK:	$P_b \approx \frac{2}{\log_2 M} Q\left(\sqrt{2\rho_b \log_2 M}\sin\left(\frac{\pi}{M}\right)\right)$
Rect. MQAM:	$P_b \approx \frac{2(\sqrt{M}-1)}{\sqrt{M}\log_2 M} Q\left(\sqrt{\frac{3\rho_b \log_2 M}{(M-1)}}\right)$
Nonrect. MQAM:	$P_b \approx \frac{4}{\log_2 M} Q\left(\sqrt{\frac{3\rho_b \log_2 M}{(M-1)}}\right)$

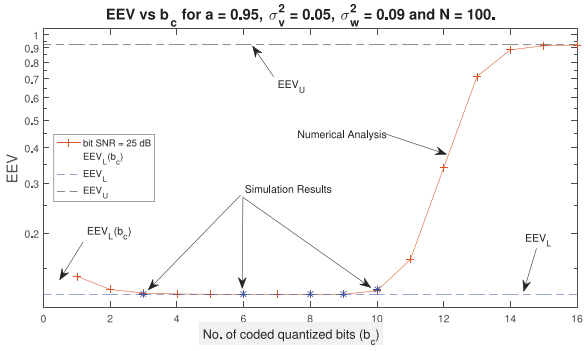

Fig. 2 *Variation of EEV as a function of b_c for a fixed SNR of 25 dB*

channels, for fair comparison of systems, same transmit power should be used.

To formulate the problem mathematically, the SQNR is typically modelled as $\Lambda = D_{\mathrm{R}} 2^{2b_c}$, where D_{R} depends on the dynamic range of the quantiser. Without loss of generality, we assume $D_{\mathrm{R}} = 1$. If a packet contains N bits and P_b denotes the BER, then the PLR is given by

$$\mathbb{P}(\gamma_k = 0) = \epsilon(b_c) = 1 - (1 - P_b(b_c))^N. \tag{8}$$

Table 1 lists the approximate BERs, P_b, as function of $M = 2^{b_c}$ for various popular signal constellations [11]. Let ρ_O be a fixed SNR per bit, then the optimisation problem is obtained by substituting $\epsilon(b_c)$ from Equation (8), Table 1 and the SQNR $\Lambda(b_c)$ to obtain

$$\begin{aligned} \min_{b_c} \quad & p^{\mathrm{CF}}(b_c) = \frac{\sigma_w^2 + (1-\epsilon(b_c))\frac{a^2\Lambda(b_c)}{\Lambda(b_c)+1} p_\infty^{tx}}{1 - a^2\frac{1+\epsilon(b_c)\Lambda(b_c)}{1+\Lambda(b_c)}} \\ \text{s.t} \quad & \rho_b \le \rho_O. \end{aligned} \tag{9}$$

We next analyse the steady state EEV to obtain some insights. Note that if $(1-a^2)p_\infty^{tx} < \sigma_w^2$ then $p^{\mathrm{CF}}(b_c)$ can be shown to be an increasing function of $\epsilon(b_c)$. Thus we get a lower bound, $\mathrm{EEV_L}(b_c)$, on $p^{\mathrm{CF}}(b_c)$ by substituting $\epsilon = 0$ in Equation (9). We have,

$$\mathrm{EEV_L}(b_c) = \frac{\sigma_w^2 + \frac{a^2\Lambda}{\Lambda+1} p_\infty^{tx}}{1 - a^2\frac{1}{1+\Lambda}}. \tag{10}$$

Moreover under the same condition $(1-a^2)p_\infty^{tx} < \sigma_w^2$, $\mathrm{EEV_L}(b_c)$ is a decreasing function of Λ. Thus letting $\Lambda \to \infty$, we have the universal lower bound as

$$\mathrm{EEV_L} = \lim_{b_c \to \infty} \mathrm{EEV_L}(b_c) = \sigma_w^2 + a^2 p_\infty^{tx}. \tag{11}$$

For the upper bound we let $\epsilon = 1$. We have,

$$\mathrm{EEV_U} = \lim_{\epsilon \to 1} p^{\mathrm{CF}}(\epsilon) = p^{\mathrm{CF}}(1) = \frac{\sigma_w^2}{1-a^2}. \tag{12}$$

Figure 2 plots the variations of EEV as b_c increases for a fixed SNR per bit of 25 dB for square QAM. Observe from the figure that the EEV first decreases and then saturates at a low value, $\mathrm{EEV_L}(b_c)$ as given by Equations (10) and (11) before sharply increasing and then saturating at a higher value, as given by Equation (12). Clearly, there is a range of b_c's for which EEV is minimised. In what follows we intend to characterise this range. We have

Algorithm 1 Find the optimal b_c's satisfying Theorem 1.

Require:	Inputs ρ_O, b_c^L, σ_w^2, σ_v^2, a and Modulation Type (MQAM/MPSK)
1:	Initialise $b_c^* \leftarrow \{\}$, $b_c \leftarrow 1$, $\epsilon(0) \leftarrow 1$, $\rho_b \leftarrow \rho_O$.
2:	Given b_c, compute the packet error probabilities $\epsilon(b_c - 1)$, $\epsilon(b_c)$) and $\epsilon(b_c + 1)$ using Equation (8) and Table 1
3:	If both Equations (13) and (14) are satisfied, then $b_c^* \leftarrow b_c \bigcup b_c^*$.
3a:	If, Equation (13) is satisfied with 'equality' $b_c \leftarrow b_c + 1$ go to Step 2.
	Else STOP.
3b:	Else, If $b_c == b_c^L$, STOP.
	Else $b_c \leftarrow b_c + 1$, and go to Step 2.

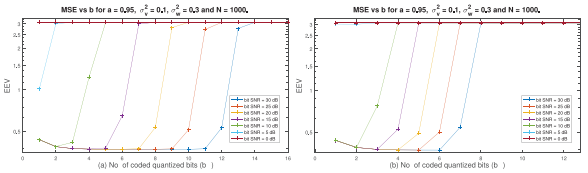

Fig. 3 *(a) Variation of EEV as a function of b_c for a fixed SNR, as SNR varies from 0–30 dB for different values of σ_w^2, σ_v^2, a and N for MQAM signal constellation in AWGN; (b)Variation of EEV as a function of b_c for a fixed SNR, as SNR varies from 0–30 dB for different values of σ_w^2, σ_v^2, a and N for MPSK signal constellation in AWGN*

Theorem 1. *The optimum values of b_c that minimise the steady-state MSE are the only b_c's that must satisfy the following simultaneously;*

$$-3\varepsilon(b_c+1)\sigma_w^2 + C_1\left[4\varepsilon(b_c+1)(\Lambda+1) - \varpi\right] \ge 0, \tag{13}$$

$$-3\varepsilon(b_c-1)\sigma_w^2 + C_1\left[4\varepsilon(b_c-1)(\Lambda+1) - \varpi\right] \ge 0, \tag{14}$$

where $C_1 = (\sigma_w^2 + (a^2-1)p_\infty^{tx})$, $\varpi = \epsilon(b_c)(1+4\Lambda)+3$.

Proof. The solution of the optimisation problem is obtained by solving the following two difference equations.

$$p^{CF}(b_c+1) - p^{CF}(b_c) \ge 0 \tag{15}$$

$$p^{CF}(b_c-1) - p^{CF}(b_c) \ge 0. \tag{16}$$

Note that $\Lambda(b_c+1) = 4\Lambda(b_c)$. Employing Equation (9) to evaluate Equations (15) and (16), and after simplification, we have Equations (13) and (14) respectively. □

Remark 1. Note that a closed-form expression for the optimal values of b_c using Equations (13) and (14) is intractable. An iterative algorithm for obtaining the optimal values is presented in Algorithm 1; wherein p_∞^{tx} can be calculated from the inputs and b_c^{L} is a preset value to stop the algorithm. Observe that when $\mathrm{EEV_L} = \mathrm{EEV_U}$ all values are optimal. When $\mathrm{EEV_L} \neq \mathrm{EEV_U}$, note that $\lim_{b_c \to 0} P_b(b_c) > 1$ for all the constellations in Table 1. So, $\epsilon(0) = 1$ and $p^{\mathrm{CF}}(0) = \mathrm{EEV_U}$. Also, as $p^{\mathrm{CF}}(\infty) = \mathrm{EEV_U}$, it follows that an optimal b_c will always exist.

Simulations and numerical results: Numerical simulation were performed to evaluate the EEV performance of the proposed system for MQAM and MPSK for both AWGN and Rayleigh Fading Channels for various values of σ_w, σ_v, N, and a. The model is simulated for 10,000 time instances and the time averaged EEV is plotted. R and C are set to 1 for simplicity. The effect of code rate R can be easily inferred by appropriately scaling with R. A coding gain of $C > 1$ results in increased cardinality of the optimal values of b_c. The numerical results are plotted with continuous line and the simulation results are marked by the blue '*' in Figure 2. Observe that the time averaged EEV is almost identical to numerical analysis results. The output of the Algorithm 1 can be inferred from the analytical plots and has been omitted.

Observe from Figure 3a that (i) the upper and lower limits vary with different values of σ_w, σ_v, and a which is as expected from (11) and (12); (ii) transition to $\mathrm{EEV_U}$ from $\mathrm{EEV_L}$ depends on N, with faster transitions as N increases; (iii) when ρ_b is greater than or equal to 10 dB, the optimal b_c's lower limit is constant. This can be justified by the observation that the lower limit of b_c depends on the quantisation noise when the SNR per bit is greater than a threshold; iv) when ρ_b is lower than a threshold, then the EEV curve is flat as the BER is poor even for low b_cs and corresponds to $(1-a^2)p_\infty^{tx} > \sigma_w^2$; This lower threshold on ρ_b can be obtained

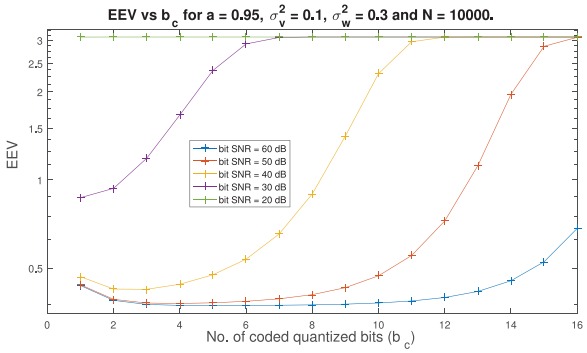

Fig. 4 *Variation of EEV as a function of b_c for a fixed SNR, as SNR varies from 20–60 dB for MQAM signal constellation in Rayleigh fading channels*

by observing that the $\epsilon(b_c) \to 1$ for the EEV to saturate at EEV_U. As in [13], summarising the values in Table 1 as $P_b(\rho_b) \approx \alpha_\text{M} Q(\sqrt{\rho_b \beta_\text{M}})$ and using (8), we have $\alpha_\text{M} Q(\sqrt{\rho_b^\iota \beta_\text{M}}) = 1 - \iota^{1/N}$, where $\iota < 1$ is a positive variable. The threshold on SNR per bit is then given by

$$\rho_b^\iota \approx \frac{1}{\beta_\text{M}} \left(Q^{-1} \left(\frac{1 - \iota^{1/N}}{\alpha_\text{M}} \right) \right)^2. \tag{17}$$

For MQAM, substituting $\iota = 0.1, b_c = 1$, and $N = 1000$ in (17), we have $\rho_b^{0.1}$ =4.28 dB. This suggests that more than 4.28 dB SNR per bit is required for the EEV optimisation to be feasible. This result corresponds well with Figure 3a where the curves for $\rho_b < \rho_b^{0.1}$ are a straight line at EEV_U. Likewise with $\iota = 0.99$, $\rho_b^{0.99} = 7.9$ dB which roughly gives the SNR per pit when the EEV curves reach EEV_L. v) the upper limit of the optimal b_c depends on the SNR per bit. As the SNR per bit increases the upper limit of optimal b_c's increases. This can be justified by the better BER as the SNR per bit increases so that the packet loss rate saturates for larger b_c's.

Figure 3b plots the variation of EEV with b_c for MPSK modulation. Observe that in addition to the inferences derived from Figures 3a and 2, the optimal range of b_c reduces while the lower limit remains constant. The reduced range is because of larger BER of MPSK as compared to MQAM which results in saturation to MSE_U for smaller b_c's. The SNR per bit threshold $\rho_b^{0.1}$ for MPSK, with $\iota = 0.1, b_c = 1$, and $N = 1000$ is 7.23 dB and $\rho_b^{0.99} = 10.2$ dB which again corresponds well with Figure 3b.

Figure 4 plots the variation of EEV with b_c for MQAM modulation over Rayleigh fading channel. Clearly, the observations made from plots in Figure 3a,b, hold but for higher SNRs. This can be explained by further degradation of average BER performance, $\bar{P}_b$ as a function of average SNR per bit, $\bar{\rho}_b$ over Rayleigh fading channels, given by [16] $\bar{P}_b(\bar{\rho}_b) \approx \frac{\alpha_\text{M}}{2}[1 - \sqrt{\frac{0.5\beta_\text{M}\bar{\rho}_b}{1+0.5\beta_\text{M}\bar{\rho}_b}}]$. There is a corresponding shift in the lower threshold on average SNR per bit which is given by

$$\bar{\rho}_b^\iota \approx \frac{2}{\beta_\text{M}} \frac{\left\{\alpha_\text{M} - 2\left(1 - \iota^{1/N}\right)\right\}^2}{\alpha_\text{M}^2 - \left\{\alpha_\text{M} - 2(1 - \iota^{1/N})\right\}^2}. \tag{18}$$

For MQAM, with $\iota = 0.1, b_c = 1$, and $N = 10,000$, $\rho_b^{0.1} = 26.27$ dB and $\rho_b^{0.99} = 49.87$ dB which corresponds well with Figure 4. Observe from all the figures that when the SNR per bit is large enough ($> \rho_b^{0.99}$) then the lower limit of optimal b_c's starts at 3 bits. Further, for such SNR's the upper limit obtained by using the Chernoff bound is very loose.

Discussion and conclusions: We have considered estimation over a lossy, capacity, and power limited channel in this letter. We have shown that there is an optimal range of quantisation bits that minimises the EEV. We have further shown that the upper and lower limits depend on the quantisation noise and BER, respectively. We have shown that these observations are equally valid for Rayleigh fading channels with higher SNRs. The SNR per bit values for which optimisation is feasible have also been provided. The results are similar for other encoder functions, $f(\cdot)$, and have been omitted. For WiFi and LTE, it has been shown that exponential curves model well the packet loss curves in AWGN and inverse SNR curves for Rayleigh channels [10]. As such, the results of this letter will also apply to these systems. Additionally, there is a possibility of various SNR levels in practical systems, which suggests a different adaptive approach to choosing the MCS for optimising the EEV. Future research directions include vector systems, power control, and coding [18].

Acknowledgment: The authors would like to thank Dr. Aaqib Patel for useful discussions on this letter.

Conflict of interest: The authors declare no conflict of interest.

Data availability statement: Data available on request from the authors

Received: *6 December 2021* Accepted: *7 June 2022*
doi: 10.1049/ell2.12558

References

1 Gupta, V., Spanos, D., Hassibi, B., Murray, R.M.: On LQG control across a stochastic packet-dropping link. In: *Proceedings of the 2005, American Control Conference*, pp. 360–365. IEEE, Piscataway, NJ (2005)
2 Sinopoli, B., Schenato, L., Franceschetti, M., Poolla, K., Sastry, S.: Optimal linear LQG control over lossy networks without packet acknowledgment. In: *Proceedings of the 45th IEEE Conference on Decision and Control*, pp. 392–397. IEEE, Piscataway, NJ (2006)
3 Ribeiro, A., Schizas, I.D., Roumeliotis, S.I., Giannakis, G.B.: Kalman filtering in wireless sensor networks. *IEEE Control Syst. Mag.* **30**(2), 66–86 (2010)
4 Xu, J., Li, J.X.: State estimation with quantized measurements in wireless sensor networks. In: *Proceedings of the 29th 2007 Chinese Control Conference (CCC)*, pp. 4857–4862. IEEE, Piscataway, NJ (2010)
5 Fu, M., de Souza, C. E.: State estimation for linear discrete-time systems using quantized measurements. *Automatica* **45**(12), 2937–2945 (2009)
6 Sinopoli, B., Schenato, L., Franceschetti, M., Poolla, K., Jordan, M., Sastry, S.: Kalman filtering with intermittent observations. *IEEE Trans. Automatic Control* **49**(9), 1453–1464 (2004)
7 Ribeiro, A., Giannakis, G., Roumeliotis, S.: SOI-KF: Distributed Kalman filtering with low-cost communications using the sign of innovations. *IEEE Trans. Signal Process.* **54**(12), 4782–4795 (2006)
8 You, K., Xie, L., Sun, S., Xiao, W.: Multiple-level quantized innovation Kalman filter. *IFAC Proc. Vol.* **41**(2), 1420–1425 (2008)
9 Dey, S., Chiuso, A., Schenato, L.: Remote estimation with noisy measurements subject to packet loss and quantization noise. *IEEE Trans. Control Netw. Syst.* **1**(3), 204–217 (2014)
10 Zhong, Y., Liu, Y.: Flexible optimal Kalman filtering in wireless sensor networks with intermittent observations. *J. Franklin Inst.* **358**(9), 5073–5088 (2021)
11 Li, Y., Chen, C.H., Wong, W.S.: Power control for multi-sensor remote state estimation over interference channel. *Syst. Control Lett.* **126**, 1–7 (2019)
12 Maass, A., Nešić, D., Varma, V., Postoyan, R., Lasaulce, S.: Stochastic stabilisation and power control for nonlinear feedback loops communicating over lossy wireless networks. In: *59th IEEE Conference on Decision and Control (CDC)*, pp. 1866–1871. IEEE, Piscataway, NJ (2020)
13 Jie, C., Gang, W., Jian, S.: Power scheduling for Kalman filtering over lossy wireless sensor networks. *IET Control Theory Appl.* **11**(4), 531–540 (2017)
14 Dey, S., Chiuso, A., Schenato, L.: Feedback control over lossy SNR-limited channels: linear encoder–decoder-controller design. *in IEEE Trans. Autom. Control* **62**(6), 3054–3061 (2017)
15 Sanjaroon, A., Farhadi, A., Khalaj, B., Motahari, A.: Estimation and stability over AWGN channel in the presence of fading, noisy feedback channel and different sample rates. *Syst. Cont. Lett.* **123**, 75–84 (2019)
16 Park, J., Han, S.: Improved remote estimation over a capacity-limited and lossy channel. *IEEE Control Syst. Lett.* **1**(2), 406–411 (2017)
17 Goldsmith, A.: Digital modulation and detection. In: *Wireless Communications*, pp. 126–171. Cambridge University Press, Cambridge (2005)
18 Quevedo, D.E., Østergaard, J., Ahlen, A.: Power control and coding formulation for state estimation with wireless sensors. *IEEE Trans. Control Syst. Tech.* **22**(2), 413–427 (2014)